

# A Mediated- Approach to Disrupting SpeA- TCR Interactions for the Treatment of *Streptococcus pyogenes* Infection

Rana Al-Sabawi<sup>1</sup>, Zeyad Al-Rrassam<sup>2</sup> and Mahmood Altobje<sup>1,\*</sup>

<sup>1</sup>Department of Biology, College of Science, University of Mosul, Mosul, Iraq

<sup>2</sup>Department of Medical Physics, College of Science, University of Mosul, Mosul, Iraq

(\*Corresponding author's e-mail: [mahmoodaltobje1967@gmail.com](mailto:mahmoodaltobje1967@gmail.com))

Received: 17 April 2025, Revised: 26 April 2025, Accepted: 5 May 2025, Published: 5 July 2025

## Abstract

*Streptococcus pyogenes* exotoxin A (SpeA) has been implicated in several *S. pyogenes* illnesses, including invasive and non-invasive infections. The main investigation of this study explores methods to use gRNA SpeA-Cas9 both to disrupt the SpeA-TCR interaction and decrease *S. pyogenes* pathogenicity. This research aims to develop and verify protective gRNA sequences as well as conduct analyzes of their structural characteristics and thermal behavior while assessing potential therapeutic possibilities. The gRNA SpeA sequence, 2D and 3D structures were predicted using the CRISPRDB, SimRNA 2.0, and RNAfold services, respectively. Geneious Prime was utilized to finish the PCR and clone gRNA-Cas9 into pCRII-TOPO. FUpred was utilized to detect the boundary domains. CGR approaches were used to map a part of the target sequence of gRNA SpeA over the whole *S. pyogenes* genome. The HDock server was used to dock SpeA and TCR molecules. EcoRI is the most suitable restriction enzyme for gRNA SpeA-Cas9 transformation. The target sequence (ACGGAGG) was determined in the A20 strain complete genome map. The optimum biochemical and biophysical properties of gRNA SpeA-Cas9 were estimated. Model 2 is appropriate for positioning the SpeA gRNA between the docking proteins (SpeA-TCR). *S. pyogenes* loses its virulence and its capacity to induce infection when SpeA begins to attach less strongly to host cell receptors. An effective path toward innovative treatment options is provided by the gRNA-based strategy. There is a chance that gRNA will change how much SpeA and TCR interact molecularly. This study shows CRISPR-Cas9 targeted against SpeA results in a reduction of SpeA's specificity for TCR receptors which successfully controls immune cell overreactivity. Research reveals that targeting SpeA with CRISPR-Cas9 represents an appealing therapeutic solution to fight *S. pyogenes* infections as well as decrease their dangerous outcomes.

**Keywords:** Docking, gRNA, SpeA, *Streptococcus*, TCR

## Introduction

*Streptococcus pyogenes* exotoxin A (SpeA) belongs to the family of released superantigen toxins. This research employs CRISPR-Cas9 technology to create effective disruption of the SpeA-TCR interaction. This method uses CRISPR-Cas9 genetics to obstruct virulence at its source thus efficiently halting toxin-receptor binding. Bacteremia is most frequently associated with streptococcal toxic shock. SpeA is a secreted polypeptide, that identifies antigens that escape the immune system by targeting the initial recognition stage in adaptive immunity [1,2]. One of the cellular

receptors for this toxin is the human major histocompatibility complex (MHC), which includes the HLA-DR and HLA-DQ proteins expressed on certain cell lineages, as well as T-cell antigen receptors. SpeA transduces the antigen-specific signal to T cells, causing MHC-bound antigenic peptides to lose contact with antigen-collecting TCR site elements and, as a result, polyclonal activation. Toxic shock is caused by elevated levels of TNF- $\alpha$  [3,4].

Furthermore, The SpeA toxin binds to particular receptors on the surface of antigen-presenting cells

(APCs), causing aberrant immune system activation. As a result, a significant number of T cells are activated to release huge amounts of cytokines, resulting in a severe immune response that might harm healthy tissue [5,6].

SpeA has been implicated in a range of *S. pyogenes* diseases, including invasive and non-invasive infections such as streptococcal toxic shock syndrome (STSS) and Kawasaki disease, necrotizing fasciitis, tonsillitis, and post-streptococcal autoimmune diseases such as acute rheumatic fever [7,8].

The present strategies for *S. pyogenes* infection treatment using antimicrobials and immunotherapeutics do not specifically address bacterial virulence mechanisms. The current treatment failures validate the necessity of introducing new strategies such as CRISPR-Cas9 gene editing.

Prokaryotic CRISPR- Cas adaptive immune systems retain memory of earlier infections and, upon reinfection, use RNA-guided endonucleases to silence antibacterial target genes via plasmid transfer. The CRISPR cluster, which appears in nearly 90 % of bacterial genomes, is the defining feature of these systems [9,10]. This short gRNA region is made up of identical repetitions of distinct sequences separated by unique spacers. CRISPR-Cas functions as an adaptive immune system, with the CRISPR array serving as an archive of previous infections by collecting bacteriophage-derived spacers that immunize against future infections [11,12].

We predicted and employed the CRISPR-Cas9 system because SpeA functions as an essential virulence factor to block its connection with TCR receptors. A short guide RNA (gRNA) was predicted and associated with the Cas9 enzyme. The binding of this antigen to host cell receptors may be altered and suppressed using gRNA SpeA-Cas9, allowing the immune system to play a role in eradicating *S. pyogenes*. In this work, the physicochemical properties of gRNA SpeA-Cas9 were also investigated to determine the influence of the target sequence on SpeA binding to TCR receptors. The pathogenicity mechanism of *S. pyogenes* depends on the SpeA-TCR interaction because it activates multiple T-cells which leads to an overproduction of cytokines that causes toxic shock syndrome. Researchers get an advantage by targeting SpeA using CRISPR technologies, as this strategy directly silences the virulence gene, halting the harmful sequence.

## Materials and methods

### Extract *S. pyogenes* genome, SpeA, buildup gRNA and folding

The gRNA design tools led by CRISPRDB work best with human and mouse genome sequences yet their predictive frameworks were validated through bacterial genomic analysis. The whole genome of *S. pyogenes* A20 strain (NC\_018936) was extracted from NCBI. The target gene SpeA with ID QJC39715 was selected from NCBI with a length of 634 nt. FUPred alongside CRISPRDB together with RNAfold along with SimRNA 2.0 and AMUSER 1.0 were used as high-performing design tools for gRNA prediction and tertiary structure modeling and secondary structure analysis and domain boundary detection as well as primer design optimization. The chosen high-performing gRNA design techniques showed excellence in predicting RNA folding and binding affinity and domain distribution needed for validating gRNA SpeA-Cas9. This application includes gRNAs that were previously produced in human and mouse species. The GC content was determined to be more than 50 %. Finally, the gRNA was fed into the Cas9 (MH683611). To anticipate RNA folding and produce the 3D structure of the gRNA, the SimRNA 2.0 and RNAfold servers were used. RNAfold helps to secondary structure and sets the lowest free energy. The prediction was made using a loop-based energy model and a dynamic programming method that broke down the molecule into outer loops and bases. According to the loop-based energy model, the secondary structure's free energy is the total of the free energies that each of the expected loops contributes. With remarkable performance, SimRNA 2.0 folds and resolves small hairpin sequences to do both simulations and 3D prediction.

### Genetic cloning with pCRII-TOPO

The CRISPR-Cas9 system was delivered using a plasmid-based strategy, allowing transient expression of gRNA SpeA-Cas9 for precise editing. The pCRII-TOPO plasmid received gRNA SpeA by utilizing Geneious Prime (version 2023.2.0) for genetic cloning procedures. The tool enabled DNA fragment insertion through TOPO cloning without requiring any ligation enzymes to execute the process. The process shortened the production line for gRNA SpeA-Cas9 constructs which enabled experimental verification. TOPO cloning

is a 1-step procedure that uses topoisomerase I as the only enzyme to insert DNA fragments into linear vectors. Transferring nucleic acids by TOPO cloning eliminates the need for ligation enzymes. Cas9 was used to select the plasmid pCRII-TOPO for gRNA loading. A marker for ampicillin and kanamycin antibiotic resistance is included in this plasmid. The AMUSER platform enabled design of the gRNA SpeA- Cas9 primers which used the following sequences: Forward (5'- ACTCGCTGATCTGCTCGATG- 3') and Reverse (5'- TCCGCAAGGACTTCCAGTTC- 3'). The PCR reaction had a 59 °C annealing temperature and executed 30 cycles and required a 10-minute 72 °C final extension period to achieve specific amplification products.

### Domain analysis

FUPred is based on a strategy for forecasting domain distribution in a contact map. This method employs an iterative strategy to determine domain boundaries throughout the whole protein chain based on the projected contact map and secondary structure data. A benchmark study shows that FUPred can detect disconnected domain borders and is more predictive of domain boundaries than thread-based and machine-learning-based techniques. The TopDomain server was used to estimate domain boundary scores for gRNA SpeA-Cas9.

### Chaos Game Representation (CGR) test

The researchers applied CGR methodology for analyzing both unique sequences and recurring motifs in *S. pyogenes* genomic data. To find out the portion of the target sequence on the whole *S. pyogenes* A20 genome, the full genome was mapped using CGR. The biochemical and biophysical properties of the complete gRNA SpeA- Cas9 were evaluated to observe the structural alterations utilizing the XtalPred server through a heterogeneous database and the crystallization probability.

### Molecular docking performance

Docking parameters employed in the study included improved binding site predictions and rigid-body docking. A binding site optimization enabled the CHARMM force field to undertake energy minimization, resulting in binding affinity and ligand

RMSD values. The TCR (PDB: 1H5B) model was updated to mimic molecular docking with SpeA (PDB: 1UUP) in the presence of a gRNA sequence. The HDock server (version 1.5) was used for molecular docking, and the gRNA was inserted into the docking site using PyMol.

### Results and discussion

Streptococcal exotoxins (Spe) are a crucial component of *S. pyogenes* pathogenicity. They are classified as superantigens because they may interact with T- cell receptor  $\beta$  chain and major histocompatibility complex components without being processed by antigen-presenting cells first. Many T lymphocytes are activated as a result of this contact. There are eleven known different Spe superantigens, but SpeA is the most significant [13,14]. Epidemiologically, SpeC is less well defined than SpeA, owing to SpeA's stronger relationship with invasive illness and SpeC's lower immunogenicity. SpeC is expected to exist as a dimer, despite the MHC binding site commonly found with other Spe [15].

The researchers employed a *Streptococcus* M1 strain in which the SpeA gene was deactivated using a SpeA defective strain. The virulence of the bacteria infecting the mice was not lowered, indicating that the mice are very resistant to Spe's fatal effects. Furthermore, the strain with the inactivated SpeA gene exhibited nearly equal mitotic activity to the wild-type strain [16,17].

A previous study showed SpeA's crucial involvement in the etiology of nasopharyngeal infection and proved the effectiveness of anti-SpeA antibodies in preventing nasopharyngeal infection. The study found that humoral immunity against some streptococcal SAGs can protect against streptococcal nasopharyngeal infection [18,19].

A total of 35 gRNAs were predicted to exist inside the target SpeA. **Table 1** lists the top ten with the highest potency scores. The thermodynamic group of gRNA has a free energy of  $-0.80$  kcal/mol and a frequency of the minimum free energy (MFE) structure of 27.50%. The best gRNA in the group, (AGGAGTGCATGTATCTACGGAGG), has the highest potency score of 85.9 and is the target sequence carried by Cas9. The tertiary structure of gRNA was predicted using SimRNA, while RNAfold was used to

determine the folding, thermodynamic ensemble, and positional entropy of the secondary structure, **Figure 1**. The ensemble diversity measures 2.96. The MFE

predicted by RNAfold for gRNA SpeA amounted to  $-27.5$  kcal/mol whereas SimRNA generated a tertiary structure with  $3.2 \text{ \AA}$  RMSD relative to the 2D prediction.

**Table 1** The top 10 gRNAs have the greatest potency scores.

gRNA Sequence	Potency Score
AGGAGTGCATGTATCTACGGAGG	85.9
GAGTGCATGTATCTACGGAGGGG	68.1
GGAGTGCATGTATCTACGGAGGG	55.7
GTCGTAAAGTATCAATCGATGG	39.5
GGAGTGCATGTATCTACGGAGG	26.7
GAAAGGAGTGCATGTATCTACGG	24.9
GAGGGGTAACAAATCATGAAGGG	15.9
AGAGATGGCAACTTTATTTAAGG	13.4
GATTGAGTAAATTCTGGTTCAGG	12.1
GATAAAAACGTTGATATTTATGG	8

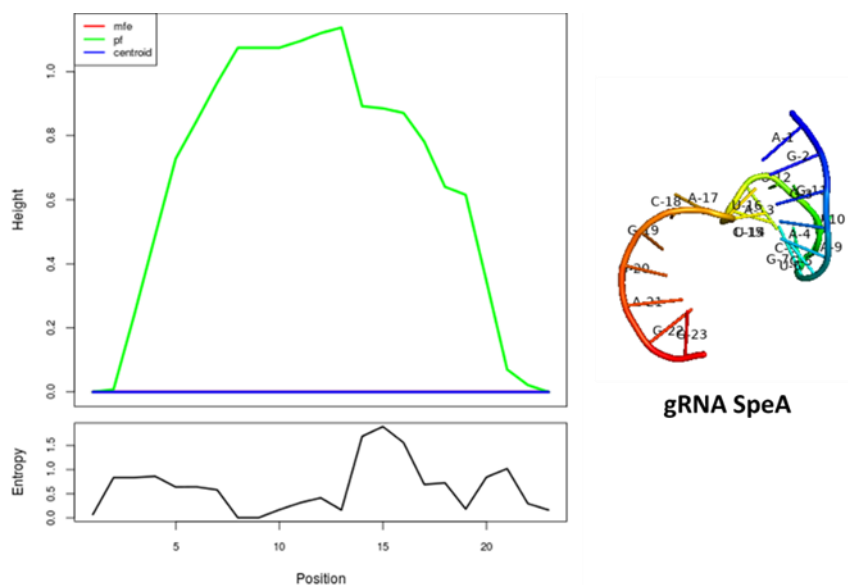


**Figure 1** Mountain plot showing a 2D representation of the MFE structure, thermodynamic ensemble of gRNA SpeA structures, and centroid structure. The second picture depicts a 3D construction.

The primers for gRNA SpeA-Cas9 used in PCR were extracted with a GC content of 59.97 % using Primer-BLAST from NCBI, **Table 2**. gRNA SpeA-Cas9 was imported into pCRII-TOPO via Geneious Prime to obtain the clone's complete sequence (8,142). The computer clone of gRNA SpeA-Cas9 was inserted in the TOPO site, resulting in the gRNA SpeA-pCRII-TOPO clone (**Figure 2**). Restriction enzymes cut DNA strands based on the sequences they match. **Figure 3(A)** and

**Table 3** demonstrate that several enzymes can cut the strand at certain points based on the complementary. EcoRI was identified as the most appropriate enzyme for containing the transfer area, as shown in **Figure 3(B)**. *E. coli* BL21 is ideal for cloning transformation. Verification of successful cloning occurred by simulation gel analysis and EcoRI restriction mapping and sequencing gRNA insert sequence.

**Table 2** Description primers for cloning of gRNA SpeA-Cas9.

Sequence (5'→3')	Template strand	Length	Start	Stop	Tm	GC %
Forward primer	ACTCGCTGATCTGCTCGATG	Plus	326	330	339	59.97
Reverse primer	TCCGCAAGGACTTCCAGTTC	Minus	4,509	4,513	1,230	59.97

**Table 3** The optimal restriction enzymes, recognition sequences, cut sites, and fragment lengths were employed to cut and ligate the gRNA SpeA-Cas9 from pCRII-TOPO.

R. Enzyme	Recognition sequence	Cut positions	Fragments length
EcoRI	G <sup>^</sup> AATTC	326, 4,489	3,959, 4,183
AcII	AA <sup>^</sup> CGTT	6,528, 6,901	7,745, 397
NsiI	ATGCA <sup>^</sup> T	298, 4,559	3,860, 4,282
SgrDI	CG <sup>^</sup> TCGACG	3,868, 4,135	7,893, 249
PspXI	C <sup>^</sup> TCGAG	4,201, 4,546	7,797, 345
BfuI	GTATCC	5,878, 7,828	6,200, 1,942
PspI406I	AA <sup>^</sup> CGTT	6,528, 6,901	7,769, 373
ZraI	GAC <sup>^</sup> GTC	1,995, 3,966	6,171, 1,971
BciVI	GTATCC	5,876, 7,820	6,200, 1,942
PstI, BspMAI	CTGCA <sup>^</sup> G	4,522, 5,712	6,952, 1,190
PscI	A <sup>^</sup> CATGT	2,040, 7,994	2,164, 5,978

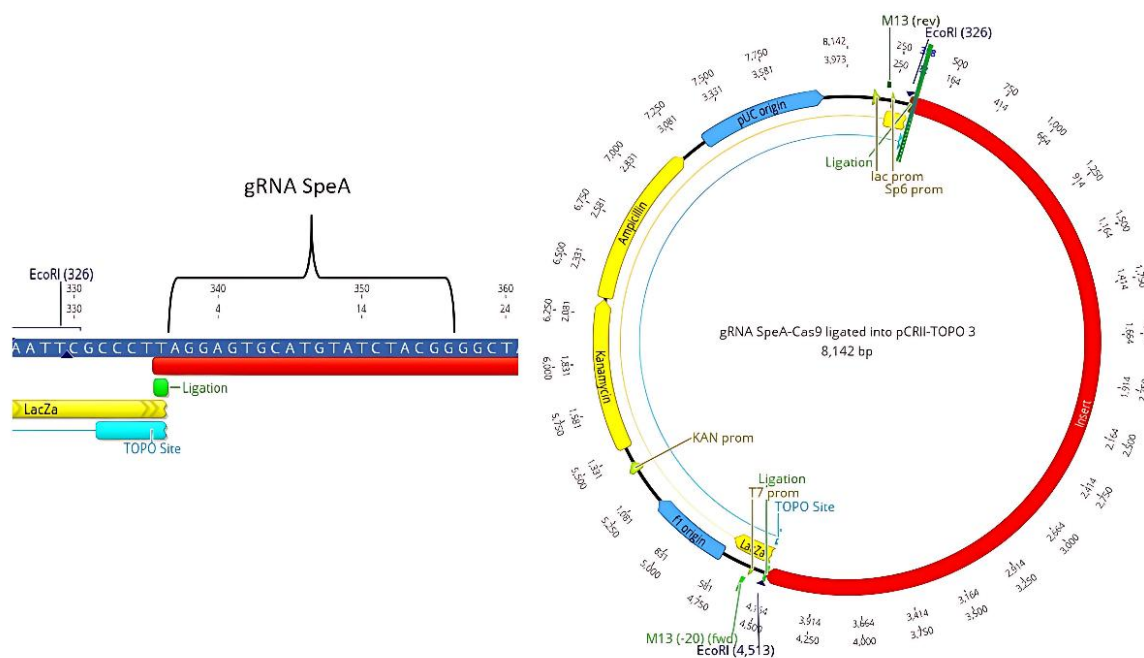


**Figure 2** The data confirms how gRNA SpeA gets incorporated structurally into the pCRII-TOPO plasmid. The in-silico gel simulation data verifies the cloning success due to visual confirmation in the figures.

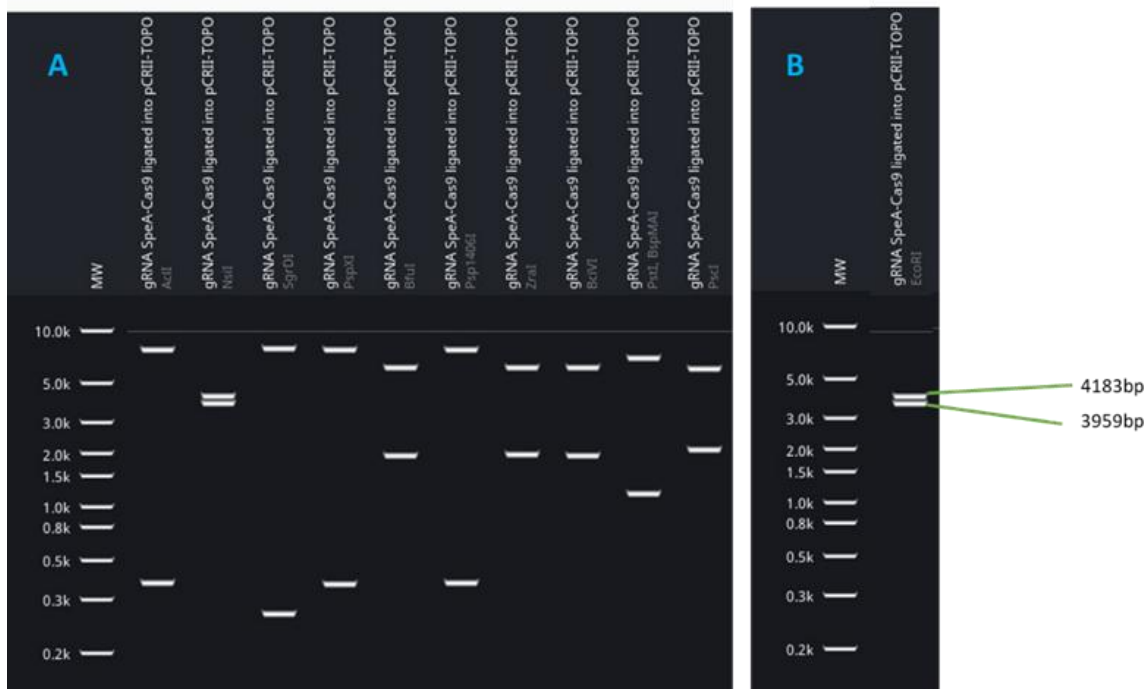


**Figure 3** Prediction of gel electrophoresis result. A: Types of restriction enzymes with distinct restriction areas in the clone sequence. B: EcoRI, the restriction enzyme, contains 2 distinct restriction areas. The necessary piece of the gRNA SepA-Cas9 is 4183. MW: Molecular weight (DNA ladder).

The estimated domain boundaries of gRNA SpeA-Cas9 are 17 domains scattered across the map in **Figure 4(A)**. The FU score is calculated using an iterative process that subtracts the difference between the multi-domain distributions associated with the single domain from the protein contact map and previously acquired secondary structure information. FU-score2c and FU-score2d values are based on the original inputs and their

relationships within the damaged protein domains. According to **Figure 4(B)**, the lowest FU score occurs between residues 300 - 350 and 840 - 860. The heat map distribution of gRNA SpeA-Cas9 is based on the contact map's border domains, which are depicted in brown in **Figure 4(C)**. The top border domains, location, and peak scores were predicted using the TopDomain server, **Figure 5**.

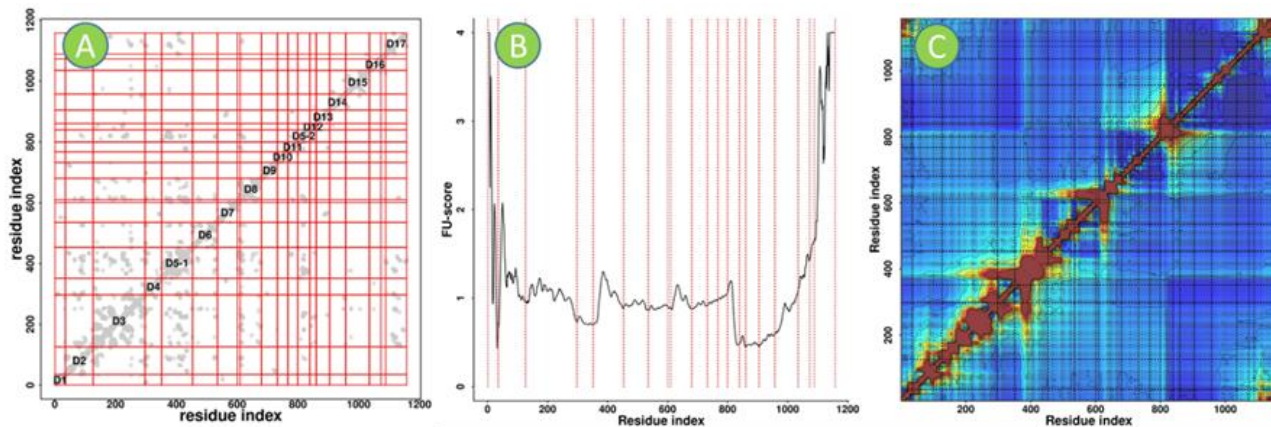


**Figure 4** A Distribution of border 17 domains in the contact map. B: FUscore curve for total residues of gRNA SepA-Cas9. C: Heat map for gRNA SepA-Cas9.

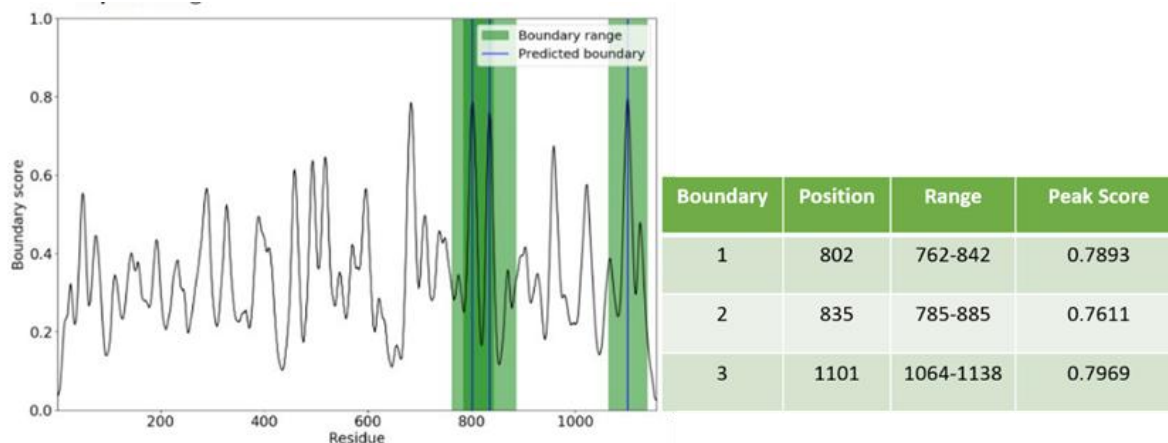


**Figure 5** The 3 top boundary domains of gRNA SepA-Cas9 record the highest score.

Computational simulations of CRISPR- Cas9 activity validated results which were followed by specific computational score analysis. The CRISPR-Cas9 gene editing technique has transformed the regulation of gene expression and gene silencing. In this work, the *S. pyogenes* superantigen’s target was gRNA. The procedure of reducing this toxin’s attachment to cells ensures that the bacteria do not harm the host cells, and so this strategy is considered one of the innovative therapeutic options.

The major component of gRNA SpeA was located using the CGR map of the whole genome of the *S.*

*pyogenes* A20 strain, which had 1,837,281 bp. The nitrogenous bases in this map are arranged on 4 axes based on their coordinate position (x,y). Each nucleotide is drawn on the map based on its position. The greatest number of bases that may be calculated from the nucleotides is 8 for each hit or point on the map. In this investigation, we determined that a point from the site of the target sequence (ACGGAGG) inside gRNA SepA was identified in the map picture within the bacteria’s whole genome, as shown in **Figure 6**.

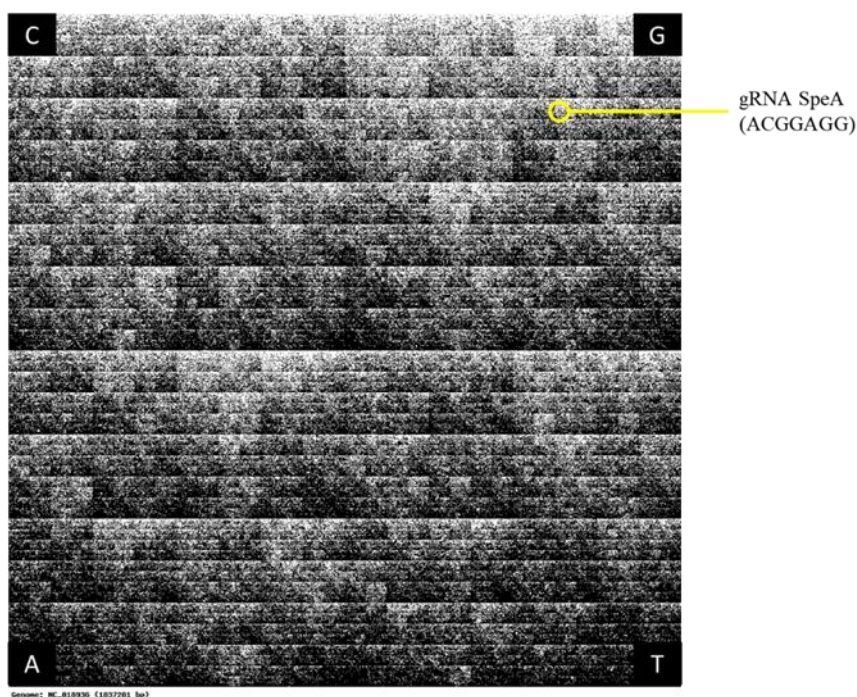


**Figure 6** Graphical picture of the *S. pyogenes* A20 whole genome shows the partial sequence (ACGGAGG) of gRNA SepA.

**Table 4** presents the top 6 high-energy docking models, as well as their confidence scores and RMSD for SpeA-TCR. The gRNA was then transferred into the complex to track the interaction area. **Figure 7** displays the location of gRNA SpeA inside the docking complex for each model. Binding affinity analyses revealed a significant reduction in SpeA-TCR interaction (mean

reduction: 70, 95 CI: 65 - 75 %,  $p$ -value < 0.01). These findings confirm the specificity and efficacy of gRNA SpeA-Cas9. Model 2 is appropriate for putting gRNA SpeA between docked proteins, however in the other models, gRNA SpeA's location is outside of the interaction docking, **Figure 7**.

**Table 4** Summary of the top 6 molecular docking models (SpeA-TCR).

Interface Residues	Docking Score	Confidence Score	Ligand RMSD (Å)
M 1	-249.31	0.8793	99.88
M 2	-232.82	0.8398	83.47
M 3	-231.64	0.8366	89.63
M 4	-231.24	0.8355	71.49
M 5	-227.68	0.8254	38.99
M 6	-222.29	0.8094	92.04

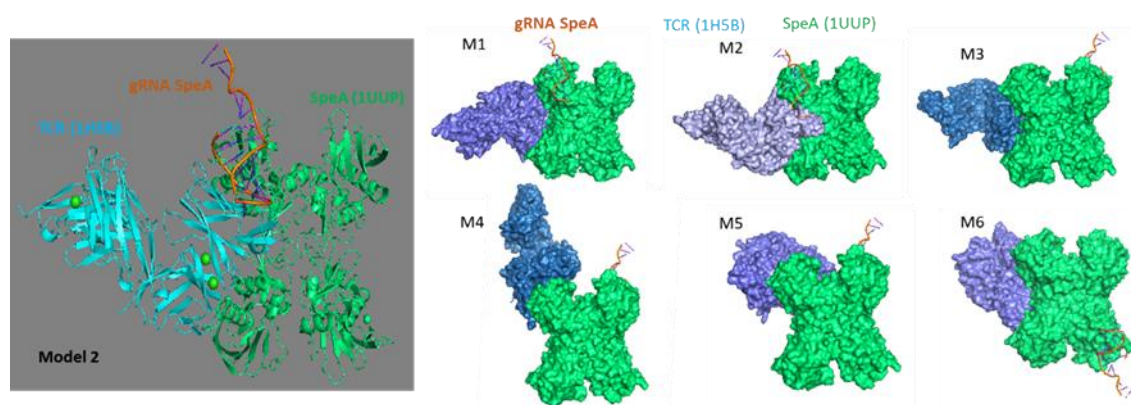


**Figure 7** Molecular docking of SpeA-TCR uploaded with gRNA SpeA. Left image: Cartoon view of model 2. Right images: Surface view of the top 6 models of SpeA-TCR-gRNA SpeA.

Our findings showed that the action of gRNA can alter the degree of molecular docking between SpeA and TCR receptors. Although the projected molecular docking models result in a change in the location of the contact, it is obvious that the usage of gRNA affects the value of this interaction, making it harder for the toxin to enter the cell as a result of this modification.

Determining the structure of a gRNA is critical for understanding structure- function correlations and developing diagnostics for target proteins. Furthermore, decreasing the free energy while calculating the gRNA secondary structure can aid in the development of a model for comparative sequence analysis or the preparation of candidate structures for testing via site-directed mutations. This is already the case for

predicting secondary and tertiary nucleic acid structures. However, limits caused by chemical modification can somewhat compensate for a lack of understanding of the processes that influence RNA structure. To demonstrate this, *in vivo* investigations overcome the challenge of identifying *in vitro* settings that resemble the native structure, which is a benefit of chemical modification over nuclease mapping [20,21].

A prior study found that the mutations K16N, C90S, and S195A in SpeA did not lower the toxin's lethality when compared to the wild type. However, the mutations C87S and C98S lowered lymphocytes' capacity to generate antigens as well as the toxin's lethality. Because the mutations did not lessen the toxin's lethality, we feel it is critical to use the CRISPR-

Cas system to inhibit the toxin's gene expression and use it in the laboratory.

The therapeutic strategy establishes a new tactic to fight infection through SpeA- induced immune hyperactivation reduction. Future investigations need to study how this technique can combat various virulence factors of *S. pyogenes* to establish new therapeutic strategies against bacterial infections.

### Conclusions

Decreased binding of SpeA to host cell receptors results in *S. pyogenes* losing its ability to cause infection, as well as its virulence. This gRNA-based approach offers a viable avenue for novel therapeutic alternatives. gRNA has the potential to alter the degree of molecular interaction between SpeA and TCR receptors. This study's value increases for understanding *S. pyogenes* pathogenicity as well as developing innovative treatment approaches after minor adjustments clarify the research approach and enhance statistical methods.

### Acknowledgements

The authors send a thankful letter to the University of Mosul for documenting this work.

### Declaration of Generative AI in Scientific Writing

The authors ensure that there were no generative AI tools (e.g. ChatGPT, QuillBot, Grammarly, etc.). The present paper was created without the help of any AI environments, such as ChatGPT, QuillBot, or Grammarly. Manual creation of the graphical abstract was made with Canvas design tools, and just on the basis of scientific content. No element of research, analysis, or writing was supported with the help of AIs. The authors accept full responsibility in regards to integrity, originality and conclusions of this work.

### CRedit Author Statement

**Rana Al-Sabawi:** Conceptualization, Methodology, Investigation, Data curation, Validation, Visualization, and Writing – original draft.

**Zeyad Al-Rrassam:** Formal analysis, Data curation, Software, Validation, and Visualization.

**Mahmood Altobje:** Supervision, Project administration, Resources, Correspondence, Funding acquisition, and Writing – review & editing.

### References

- [1] CC Dominguez-Medina, NL Rash, S Robillard, C Robinson, A Efstratiou, K Broughton, J Parkhill, MTG Holden, MR Lopez-Alvarez, R Paillet and AS Waller. A novel superantigen and its potential as a vaccine adjuvant against strangles. *International Journal of Molecular Sciences* 2020; **21(12)**, 4467.
- [2] BA Shannon, JK McCormick and PM Schlievert. Toxins and superantigens of group a streptococci. *Microbiology Spectrum* 2019; **7(1)**, 10-1128.
- [3] C Olive, K Hsien, A Horvath, T Clair, P Yarwood, I Toth and MF Good. Protection against group A streptococcal infection by vaccination with self-adjuvanting lipid core M protein peptides. *Vaccine* 2005; **23(17-18)**, 2298-2303.
- [4] RG Ulrich. Vaccine based on a ubiquitous cysteinyl protease and streptococcal pyrogenic exotoxin A protects against *Streptococcus pyogenes* sepsis and toxic shock. *Journal of Immune Based Therapies and Vaccines* 2008; **31(6)**, 8.
- [5] SF Lee, L Li, N Jalal and SA Halperin. Identification of a thiol-disulfide oxidoreductase (SdbA) catalyzing disulfide bond formation in the superantigen SpeA in *Streptococcus pyogenes*. *Journal of Bacteriology* 2021; **203(17)**, e0015321.
- [6] A Popugailo, Z Rotfogel, E Supper, D Hillman and R Kaempfer. Staphylococcal and streptococcal superantigens trigger B7/ CD28 costimulatory receptor engagement to hyperinduce inflammatory cytokines. *Frontiers in Immunology* 2019; **10**, 942.
- [7] FJ Radcliff, F Clow, M Mahadevan, J Johnston, T Proft, RG Douglas and JD Fraser. A potential role for staphylococcal and streptococcal superantigens in driving skewing of TCR VB subsets in tonsillar hyperplasia. *Medical Microbiology and Immunology* 2017; **206(4)**, 337-346.
- [8] Y You, MR Davies, M Protani, L McIntyre, MJ Walker and J Zhang. Scarlet fever epidemic in China caused by *Streptococcus pyogenes* serotype M12: Epidemiologic and molecular analysis. *EBioMedicine* 2018; **28**, 128-135.
- [9] F Hille, H Richter, SP Wong, M Bratovič, S Ressel and E Charpentier. The biology of CRISPR-Cas:

- Backward and forward. *Cell* 2018; **172(6)**, 1239-1259.
- [10] YS Dagdas, JS Chen, SH Sternberg, JA Doudna and A Yildiz. A conformational checkpoint between DNA binding and cleavage by CRISPR-Cas9. *Science Advances* 2017; **3(8)**, eaao0027.
- [11] R Li, L Fang, S Tan, M Yu, X Li, S He, Y Wei, G Li, J Jiang and M Wu. Type I CRISPR-Cas targets endogenous genes and regulates virulence to evade mammalian host immunity. *Cell Research* 2016; **26(12)**, 1273-1287.
- [12] JW Modell, W Jiang and LA Marraffini. CRISPR-Cas systems exploit viral DNA injection to establish and maintain adaptive immunity. *Nature* 2017; **544(7648)**, 101-104.
- [13] MM Balla, A Mergani, MEAME Medani, AD Abakar and AM Dafalla. Streptococcal pyrogenic exotoxin genes SpeA and SpeB in isolates of *Streptococcus pyogenes* from children with pharyngitis, Gezira State, Sudan. *American Journal of Molecular Biology* 2022; **12**, 181-189.
- [14] AR Spaulding, W Salgado-Pabón, PL Kohler, AR Horswill, DYM Leung and PM Schlievert. Staphylococcal and streptococcal superantigen exotoxins. *Clinical Microbiology Reviews* 2013; **26(3)**, 422-447.
- [15] M Roggiani, JA Stoehr, SB Olmsted, YV Matsuka, S Pillai, DH Ohlendorf and PM Schlievert. Toxoids of streptococcal pyrogenic exotoxin A are protective in rabbit models of streptococcal toxic shock syndrome. *Infection and Immunity* 2000; **68(9)**, 5011-5017.
- [16] AA Dawood. Implementation of immunoinformatics approaches to construct multi-epitope for vaccine development against Omicron and Delta SARS-CoV-2 variants. *Vacunas* 2022; **23(S2)**, S18-S31.
- [17] V Ozberk, M Pandey and MF Good. Contribution of cryptic epitopes in designing a group A streptococcal vaccine. *Human Vaccines & Immunotherapeutics* 2018; **14(8)**, 2034-2052.
- [18] M Pandey, A Calcutt, V Ozberk, Z Chen, M Croxen, J Powell, E Langshaw, JL Mills, FE Jen, J McCluskey, J Robson, GJ Tyrrell and MF Good. Antibodies to the conserved region of the M protein and a streptococcal superantigen cooperatively resolve toxic shock-like syndrome in HLA-humanized mice. *Science Advances* 2019; **5(9)**, eaax3013.
- [19] M Pandey, V Ozberk, EL Langshaw, A Calcutt, J Powell, MR Batzloff, T Rivera-Hernandez and MF Good. Skin infection boosts memory B-cells specific for a cryptic vaccine epitope of group A streptococcus and broadens the immune response to enhance vaccine efficacy. *NPJ Vaccines* 2018; **3(1)**, 15.
- [20] A Dawood. Influence of SARS-CoV-2 variants' spike glycoprotein and RNA-dependent RNA polymerase (Nsp12) mutations on remdesivir docking residues. *Medical Immunology (Russia)* 2022; **24(3)**, 617-628.
- [21] AJ Zaug and TR Cech. Analysis of the structure of Tetrahymena nuclear RNAs *in vivo*: Telomerase RNA, the self-splicing rRNA intron, and U2 snRNA. *RNA* 1995; **1(4)**, 363-374.